[3]A. L. Schawlow, in *Quantum Electronics* (Columbia U. P., New York, 1960).
[4]P. Kisliuk, A. L. Schawlow, and M. D. Sturge, in *Advances in Quantum Electronics* (Columbia U. P., New York, 1964), p. 725.
[5]P. Kisliuk and W. F. Krupke, J. Appl. Phys. 36, 1025 (1965).
[6]P. Kisliuk and W. F. Krupke, Appl. Phys. Letters 3, 215 (1963).
[7]P. Kisliuk, N. C. Chang, P. L. Scott, and M. H. L. Pryce, Phys. Rev. 884, 367 (1969).
[8]A. A. Kaplyanskii and A. K. Przhevuskii, Dokl. Akad. Nauk. SSSR 142, 313 (1962) [Sov. Phys. Doklady 7, 37 (1962)].
[9]L. F. Mollenauer and A. L. Schawlow, Phys. Rev. 168, 309 (1968).
[10]G. F. Imbusch (private communication).
[11]A similar method was used almost twenty years ago by A. Schmillen to measure the fluorescent lifetimes of certain organic substances. See A. Schmillen, Z. Physik 135, 294 (1953).
[12]G. F. Imbusch, Phys. Rev. 153, 326 (1966).
[13]Stephen F. Jacobs, The Johns Hopkins Spectroscopic Report No. 24, 1969 (unpublished).
[14]S. Geschwind, G. E. Devlin, R. L. Cohen, and S. R. Chinn, Phys. Rev. 137, A1087 (1965).
[15]For a further discussion of energy transport mechanisms in ruby, see R. J. Birgenau, J. Chem. Phys. 50, 4282 (1969).

PHYSICAL REVIEW B VOLUME 7, NUMBER 4 15 FEBRUARY 1973

Phonons in Solid Hydrogen and Deuterium Studied by Inelastic Coherent Neutron Scattering

M. Nielsen
Atomic Energy Commission, Research Establishment Risö, DK-4000 Roskilde, Denmark
(Received 14 January 1972; revised manuscript received 18 September 1972)

Phonon dispersion relations have been measured by coherent neutron scattering in solid para-hydrogen and ortho-deuterium. The phonon energies are found to be nearly equal in the two solids, the highest energy in each case lying close to 10 meV. The pressure and temperature dependence of the phonon energies have been measured in ortho-deuterium and the lattice change determined by neutron diffraction. When a pressure of 275 bar is applied, the phonon energies are increased by about 10%, and heating the crystal to near the melting point decreases them by about 7%. The densities of states, the specific heats, and the Debye temperatures have been deduced and found to be in agreement with the published experimental results. The Debye temperatures are 118 K for hydrogen and 114 K for deuterium. For hydrogen the Debye-Waller factor has been measured by incoherent neutron scattering and it corresponds to a mean-square displacement of the hydrogen molecules of 0.48 Å^2.

I. INTRODUCTION

Solid H_2 and D_2 belong to the class of quantum solids (He, H_2, D_2) for which the kinetic energy of the zero-point motion of the particles is comparable with the potential energy, and the amplitudes of vibrations at 0 K are not small compared with the separation of neighboring particles.

The standard methods of lattice dynamics are not applicable to quantum solids, but new methods have been developed and theoretical predictions of the dynamical properties have been published.[1] Most of the theoretical and experimental work in this field has been concentrated on solid He.[2] However, solid H_2 and D_2 are suitable substances for studying the quantum effects because they have a large difference in isotopic mass while their intermolecular potentials are nearly identical, and in addition, they are good materials for neutron scattering experiments.

The forces between the particles in the quantum solids are of the van der Waals type and the pair potentials, which are of the Lennard-Jones form, have parameters which are fairly well known from the properties of the gas phases. Owing to the large zero-point motion and the hard-core repulsion in the pair potential at small separations, the crystals are expanded and the distance between the neighboring particles is considerably larger than the distance corresponding to the minimum in the pair potential. Furthermore, short-range correlations in the motion of the particles must be introduced to prevent overlap of the single-particle wave functions in the hard-core region of the pair potential.

To account for the short-range correlations in the ground-state wave function Nosanow[3] introduced a Jastrow factor

$$f(R) = e^{-Cv(R)/2} , \tag{1}$$

where $v(R)$ is the gas-phase pair potential and C is a variational parameter. In calculating the dynamical properties, the short-range correlations are taken into account by replacing $v(R)$ by an effective potential,

$$W(R) = f^2(R)\left(v(R) - \frac{\hbar^2}{2M}\nabla^2 \ln f(R)\right) . \tag{2}$$

The phonon energies may then be found by the standard method of lattice dynamics if the force constants are calculated as the thermal average of the second derivative of $W(R)$.

The phonon energies in solid H_2 and D_2 have been calculated by Klein and Koehler[4] and by Biem and Mertens.[5] In both calculations the potentials derived from the gas-phase properties are the only physical quantities which are used, and the comparison with the experimental results is therefore a critical test of the theories. Experimentally the phonon energies in H_2 and D_2 have been studied by Raman scattering[6] and by neutron scattering.[7,8] We have previously presented the results of coherent neutron scattering experiments on solid D_2.[8] This study has now been extended to include the pressure and temperature dependence of the phonon energies in D_2. Further we present here the first results on coherent neutron scattering in solid H_2.

The rotational quantum numbers J of the H_2 and D_2 molecules remain good quantum numbers in the solid phases. Both H_2 and D_2 exist in ortho- and para-modifications. Ortho-hydrogen (o-H_2) and para-deuterium (p-D_2) have odd quantum numbers J and para-hydrogen and ortho-deuterium have even quantum numbers J. The crystal structures of solid o-D_2 and p-H_2 are hexagonal close packed at all temperatures of the solid phases. The conversion of o-H_2 and p-D_2 takes place very slowly; 1.9% per hour in solid H_2 and 0.11% per hour in solid D_2.

The neutron scattering cross sections depend on the rotational states and this is a very important factor, especially in solid H_2 where the atomic cross section is dominated by a large spin-incoherent cross section ($\sigma_i = 79.9$ b, $\sigma_c = 1.79$ b). The differential cross sections may be expressed as[9]

$$\frac{d^2\sigma}{d\Omega d\epsilon} = N\frac{k}{k_0}\frac{1}{\pi\hbar} f_{J\to J'}(\tfrac{1}{2}\kappa d) \times \int \exp\left\{i\left[\vec{\kappa}\cdot\vec{r} - \left(\omega - \frac{E_{J'} - E_J}{\hbar}\right)t\right]\right\} G_S(\vec{r},t)\, d\vec{r}\, dt \tag{3}$$

for incoherent scattering, in which the molecular rotational quantum number is changed from J to J', and

$$\frac{d^2\sigma}{d\Omega d\epsilon} = N\frac{k}{k_0}\frac{1}{\pi\hbar}\sigma_c j_0^2(\tfrac{1}{2}\kappa d) \times \int e^{i(\vec{\kappa}\cdot\vec{r}-\omega t)} G(\vec{r},t)\, d\vec{r}\, dt \tag{4}$$

for coherent scattering, in which J retains the value of zero.

Here $\hbar\vec{\kappa} = \hbar(\vec{k}_0 - \vec{k})$ and $\hbar\omega = (k_0^2 - k^2)/(2M)$ are the momentum and energy transfers from the neutron to the solid, E_J and $E_{J'}$ are the rotational energies of the molecules with rotational numbers J and J', $G(r,t)$ and $G_S(r,t)$ are the total-correlation and the self-correlation functions, describing the motion of the centers of mass of the molecules.

The remaining functions in Eqs. (3) and (4) are defined as

$$f_{0\to 1} = 3\sigma_i j_1^2(\tfrac{1}{2}\kappa d),$$

$$f_{1\to 0} = \tfrac{1}{3}\sigma_i j_1^2(\tfrac{1}{2}\kappa d),$$

$$f_{1\to 1} = \tfrac{2}{3}\sigma_i [j_0^2(\tfrac{1}{2}\kappa d) + 2j_2^2(\tfrac{1}{2}\kappa d)],$$

where $j_i^2(\frac{1}{2}\kappa d)$ are the spherical Bessel functions and d is the distance between the nuclei in a molecule.

Equation (4) resembles the usual cross section for a monoatomic solid, except for the factor $4j_0^2(\frac{1}{2}\kappa d)$, which accounts for the spatial extension of the molecule. The incoherent cross section given by Eq. (3) is also analogous to the expression for a monoatomic solid, apart from the form factors $f_{J\to J'}$ and a shift of the energy scale of $E_{J'} - E_J$. In pure p-H_2 with $J=0$, there is no incoherent scattering as long as the energy transfer is below the rotational energy, $E_{J=1} - E_{J=0} = 14.6$ meV. As the total energy width of the phonon spectrum is about 10 meV it is possible to measure the phonon dispersion curves in p-H_2 by coherent neutron scattering without being disturbed by any incoherent scattering. In addition, the form factor for the incoherent scattering produced by the $J=0$ to $J=1$ transitions is proportional to $j_1^2(\frac{1}{2}\kappa d)$, which is small in the region where the coherent scattering is strong.

II. EXPERIMENTAL

We have concentrated our investigations on coherent neutron scattering from solid D_2 and H_2, using a triple-axis neutron spectrometer. We have only made use of incoherent scattering in the measurement of the Debye–Waller factor in H_2. In our measurements we have determined the phonon dispersion curves, which can be compared directly with the corresponding calculated curves. The samples were single crystals of pure $J=0$ phases. The measurements were performed on three different kinds of crystals, namely, crystals of solid o-D_2 at the saturated vapor pressure, o-D_2 at 275 bar, and p-H_2 at the saturated vapor pressure. In each case several crystals of the same kind were used.

The D_2 crystals were obtained by annealing polycrystalline samples at a temperature close to the melting point for several days. The crystal growth was followed by observing the neutron Bragg scattering from various grains. The resulting samples contained single crystals as large as 1 cm^3 and measurements were made on these, while carefully shielding the rest of the sample with cadmium.

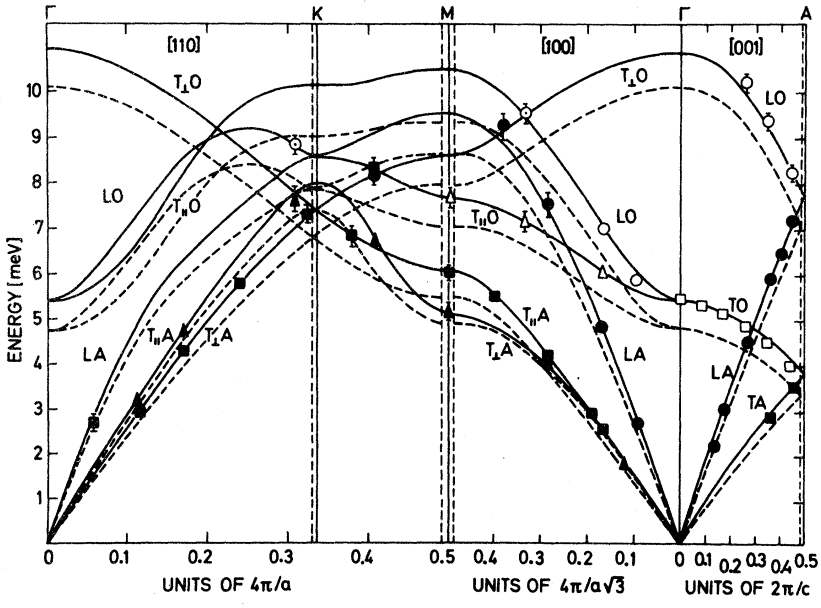

FIG. 1. Phonon dispersion relations for o-D_2 at 5 K and 275 bar. The full lines are the results of the Born–von Karman fit and the dashed lines are the dispersion relations for o-D_2 at 5 K and zero pressure.

The H_2 crystals were grown by an improved technique and single crystals as large as 40 cm^3 were obtained. The sample tube was a 2.5-cm-diam quartz tube, 12 cm long. The crystals were grown by slowly cooling the liquid-hydrogen-filled tube from the bottom, and the growth was followed visually by looking through windows in the cryostat. Grain boundaries are easily seen by means of polaroids. Several single crystals occupying the entire sample tube have been grown.

The ortho-para conversion of the hydrogen molecules was accomplished by passing the hydrogen gas through a catalyst of ferric oxide gel cooled to liquid-hydrogen temperature, before the gas was liquefied in the sample tube. In addition the upper 2 cm of the sample tube were almost filled with the same catalyst and the condensation was performed very slowly over a period of about 24 h.

III. RESULTS

A. Ortho-Deuterium

The dispersion relations in the symmetry directions were measured in o-D_2 at $T = 5$ K at the saturated vapor pressure.[8] The data were fitted to a third-neighbor general-force model,[10] and the effective-force constants obtained showed that the bond-stretching forces between nearest-neighbor molecules are dominant. The density of states and the heat capacity were calculated, and the Debye temperature was found to be $\Theta_D(0) = 114$ K. The measured dispersion curves were compared with theoretical curves calculated by Klein and Koehler,[4] and good agreement was found with their self-consistent frequencies $\omega_{\vec{q}}$. However, when short-range correlations are important, the phonon energies are usually identified as being the inverse eigenvalues $\Omega_{\vec{q}}$ of the displacement-correlation function (Ref. 4). For the highest energies, $\Omega_{\vec{q}}$ are about 20% higher than $\omega_{\vec{q}}$.

For o-D_2 at 5 K and 275 bar the measured phonon energies are shown in Fig. 1, and typical neutron groups are shown in Fig. 2. The full curves in Fig. 1 show a Born–von Karman fit to the results using a third-nearest-neighbor tensor-force model.[10] The resulting effective-force constants are shown in Table I. We have used these constants to calculate the density-of-states function, the specific heat, and the Debye temperature Θ_D. The latter two are shown in Fig. 3, together with the corresponding curves for o-D_2 at the saturated vapor pressure.

The elastic constants are calculated from the force constants, with the exception of c_{13}, which is found from the relation[11]

$$c_{11} + c_{12} = c_{33} + c_{13} + \beta_2 \Delta \ , \qquad (5)$$

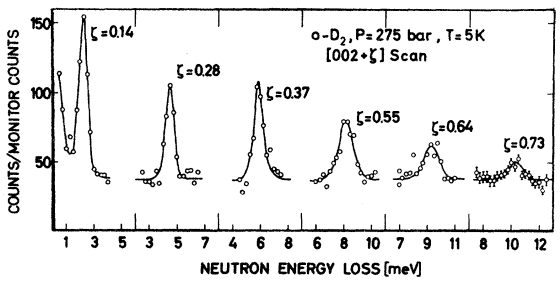

FIG. 2. Neutron groups obtained in constant $\vec{\kappa}$ scans for longitudinal phonons in the c direction in o-D_2 at 5 K and 275 bar.

TABLE I. Third-nearest-neighbor force model for o-D_2 at 5 K and 275 bar. The numbers in parenthesis are the force constants for o-D_2 at 5 K and zero pressure.

Neighbor	Coordinate of typical molecule	Force constant matrix elements (dyn/cm)				
1	$(a/\sqrt{3}, 0, \frac{1}{2}c)$	α_1	0	δ_1	α_1	84 (63)
		0	β_1	0	β_1	−17 (−9)
		δ_1	0	γ_1	γ_1	149 (127)
					δ_1	•••
2	$(0, a, 0)$	α_2	ϵ_2	0	α_2	−2 (6)
		$-\epsilon_2$	β_2	0	β_2	217 (174)
		0	0	γ_2	γ_2	−8 (−9)
					ϵ_2	17 (11)
3	$(-2a/\sqrt{3}, 0, \frac{1}{2}c)$	α_3	0	δ_3	α_3	1 (−2)
		0	β_3	0	β_3	5 (4)
		δ_3	0	γ_3	γ_3	3 (1)
					δ_3	•••

where $\beta_2 = -d \ln (c/a)/dP$ and $\Delta = c_{33}(c_{11}+c_{12}) - 2c_{13}^2$. The lattice constants a and c are determined by neutron diffraction and $\beta_2 = 0$ because the lattice is found to be strained uniformly at 275 bar. The elastic constants obtained in this way are given in Table II. The sound velocities shown in Table II are also calculated by means of the elastic constants and agree with the initial slopes of the acoustic dispersion curves.

Using the diffraction data we find the inverse compressibility constant $B = 43\times10^8$ dyn/cm^2. B may also be calculated using the elastic constants, and the values found at low pressure and at 275 bar are shown in Table II. The discrepancy between the B values obtained by these two methods lies only just outside the experimental uncertainty in the determination of the relative change of lattice constants on the application of pressure.

From the data in Fig. 1 we can find the micro-

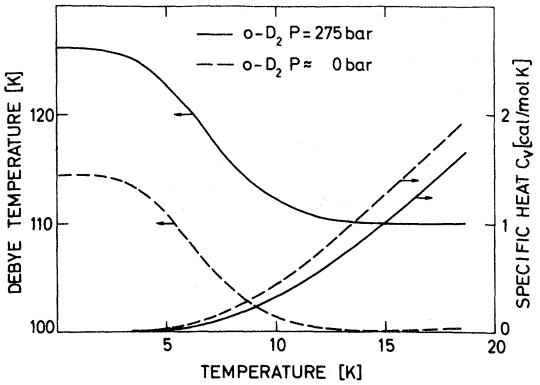

FIG. 3. Specific heat and Debye temperature for o-D_2. The functions are calculated by using the effective force constants obtained in the Born–von Karman fit to the measured phonon energies.

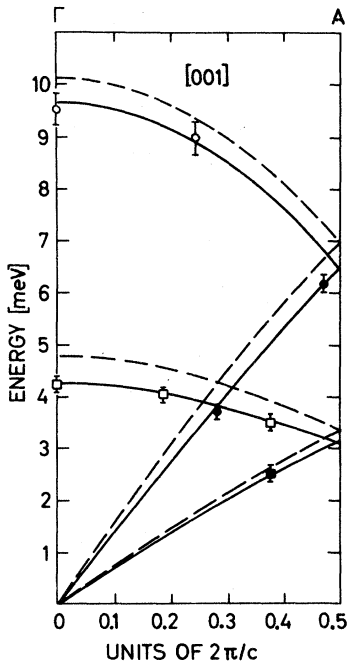

FIG. 4. Phonon dispersion relations in the c direction for o-D_2 at 18 K and zero pressure. The dashed lines are the dispersion relations for o-D_2 at 5 K and zero pressure.

scopic Grüneisen parameters $\gamma_{\vec{q}} = (\Delta\omega_{\vec{q}}/\omega_{\vec{q}})/(\Delta\rho/\rho)$, where $(\Delta\omega_{\vec{q}}/\omega_{\vec{q}})$ is the relative change of the energy of the phonon with wave vector $\vec{q}$ when the relative change of the density of the crystal is $\Delta\rho/\rho$. The experimental accuracy does not allow a detailed analysis, but an average Grüneisen parameter can be found for some of the branches of the phonon dispersion relations. For the transverse and longitudinal branch in the c direction we find

$$\gamma_T = 1.8 \text{ and } \gamma_L = 1.3 ,$$

where the density change obtained by neutron diffraction has been used. It is noteworthy that the transverse phonon energies are more sensitive to density changes than the longitudinal energies.

TABLE II. Elastic constants, sound velocities, and lattice parameters for o-D_2 at 5 K and 275 bar. The corresponding values for o-D_2 and zero pressure are shown in parentheses.

Elastic constants (10^3 dyn/cm^2)			Sound velocities (10^3 m/sec)		Lattice parameters (Å)	
C_{11}	100	(82)	v_L^z	2.38 (2.25)	a	3.526 (3.607)
C_{12}	45	(29)	v_T^z	1.18 (1.07)	c	5.750 (5.877)
C_{33}	122	(102)	v_L^{xy}	2.16 (2.02)		
C_{44}	30	(23)	v_T^{xy}	1.13 (1.14)		
C_{13}	23	(9)				
B	56	(40)				

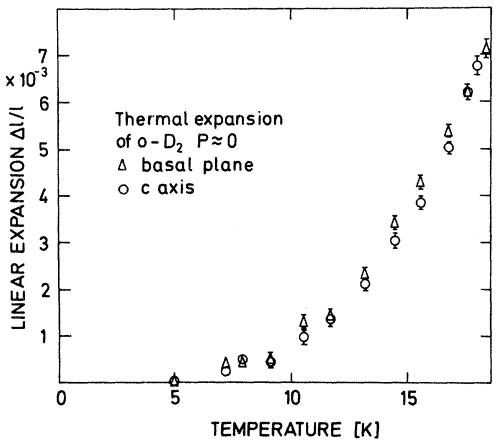

FIG. 5. Thermal expansion of o-D_2 at zero pressure measured by neutron diffraction. Within the experimental accuracy there is no difference between the expansion in the c direction and in a direction perpendicular to this.

In order to investigate the temperature dependence of the phonon energies we have measured the dispersion curves in the c direction for an o-D_2 crystal at 18 K and at the saturated vapor pressure. The result is shown in Fig. 4. The decrease in energy for the longitudinal phonon branch is $(\Delta\omega_{\vec{q}}/\omega_{\vec{q}})_{LO} = 6 \pm 2\%$ and for the transverse branch $(\Delta\omega_{\vec{q}}/\omega_{\vec{q}})_{TO} = 9 \pm 2\%$.

With the sample at the saturated vapor pressure we have also measured the thermal expansion in the c direction and in the a direction by neutron diffraction, and the results are shown in Fig. 5. Within the experimental uncertainty there is no difference between the thermal expansion in the two directions. The linear expansion data follow the power law $(\Delta l/l) = 10^{-3}(T/10\ \mathrm{K})^{3.3}$.

In a simple model where we suppose that the temperature renormalization of the phonon energies is governed by the change of the density, we may compare the microscopic Grüneisen parameters with the corresponding parameters $p = (\Delta\omega_{\vec{q}}/\omega_q)/(\Delta\rho/\rho)$, where $\Delta\rho/\rho$ is the relative density change due to thermal expansion. At $T = 18$ K we find for the transverse and the longitudinal phonons in Fig. 4 that $p_T = 4.5$ and $p_L = 3.0$. This means that for a given increase in density of o-D_2, a change of temperature results in approximately twice the change in phonon energies as is produced by increasing the pressure.

Silvera *et al.* have measured the energy of the low-lying optical phonon mode in H_2 and D_2 by Raman scattering.[6] In p-D_2 they find that the energy decreases 4.8%, when the temperature is increased from 4.2 to 14.2 K. If we assume that p-D_2 has the same thermal expansion as that of o-D_2, the corresponding change of density may be found from Fig. 4 to be 0.9%, giving $p_T = 5.3$ for p-D_2, to be compared with our value of $p_T = 4.5$ for o-D_2. Silvera *et al.* have pointed out that a faster temperature variation in p-D_2 than in o-D_2 can be explained by a short-range orientational order in p-D_2 caused by the electrical quadrupole forces between the p-D_2 molecules.

B. Para-Hydrogen

The hydrogen crystals consist of nearly pure para-hydrogen since in equilibrium at the normal boiling point 99.8% of the molecules are in their ground state $J = 0$. The neutron scattering from the

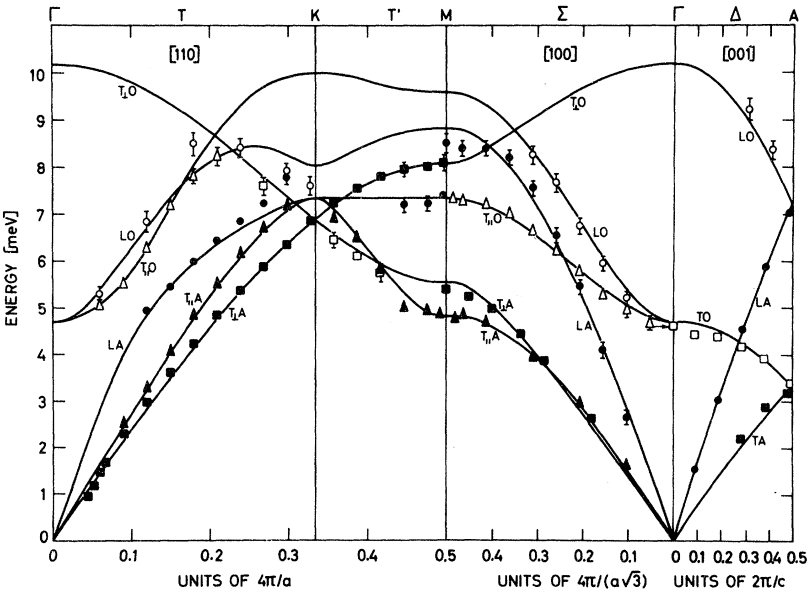

FIG. 6. Phonon dispersion relations for p-H_2 at 5.4 K and zero pressure. The full lines are the results of the Born–von Karman fit where a third-nearest-neighbor general-force model is used. The arrow at Γ shows the frequency of the TO mode as derived from Raman spectroscopy (Ref. 6).

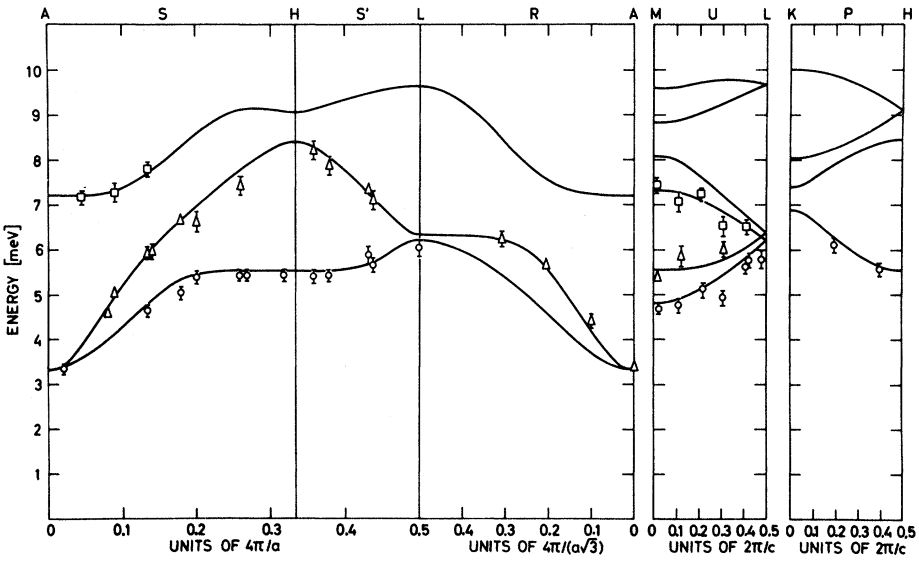

FIG. 7. Phonon dispersion relations along the Brillouin-zone boundaries for p-H_2 at 5.4 K and zero pressure. The full lines are the results of the Born–von Karman fit including the data in Figs. 6 and 7.

crystal is therefore predominantly coherent as long as the scattered energy is too low to excite the first rotational transition at 14.7 meV. However, special precautions must be taken to suppress the higher-order contamination of the monochromatic incoming neutron beam, because the higher-order neutrons are scattering strongly through the incoherent cross section of the hydrogen atoms and give rise to a high background. In the measurement we have used either a graphite crystal and a graphite filter or a germanium crystal and a quartz filter in the monochromator, and most of the measurements were performed with a fixed incoming neutron energy of 14.6 meV.

The measured phonon energies are shown in Figs. 6 and 7. The curves in the figures are the fitted Born–von Karman curves, in which a third-nearest-neighbor tensor-force model[10] has been used. Three different crystals have been used in the measurements, two crystals with the c axis nearly vertical and a third crystal with the c axis nearly horizontal, and in all three cases the crystals extended through almost the entire sample tube. The temperature was 5.4 K and the pressure zero (i.e., the saturated vapor pressure).

At the highest phonon energies there are no experimental points in Fig. 6 because it appeared impossible to obtain well-defined neutron groups. The intensity of the measured neutron groups decreases very rapidly with energy, because it is necessary to use a low incoming neutron energy to avoid incoherent scattering; in addition a strong anomalous intensity variation has been observed. Figure 8 shows the neutron groups measured for longitudinal phonons with wave vectors in the c direction, measured with a fixed analyzer energy of 4.8 meV. Due to the high relative background, the determination of the width of the neutron groups is rather uncertain. However, the phonons are not heavily damped, the natural widths [full width at half-maximum (FWHM)] being no larger than 10% of the phonon energies. The neutron groups are ap-

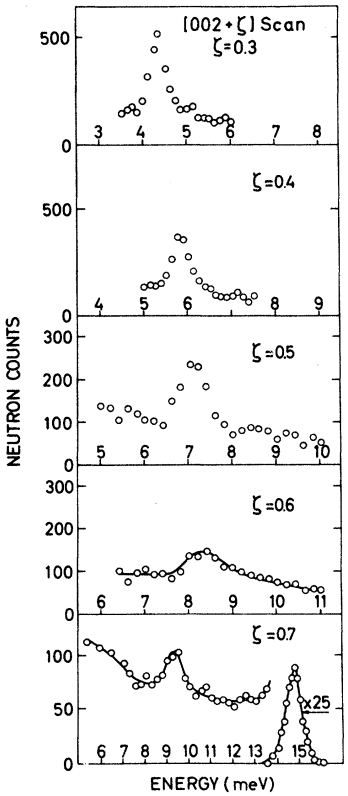

FIG. 8. The measured neutron groups for longitudinal phonons with wave vectors in the c direction in p-H_2. The analyzer energy was fixed at 4.8 meV.

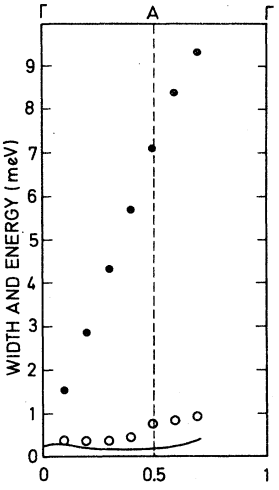

FIG. 9. The widths (open circles, FWHM) and the energies (full circles) of the measured neutron groups for the longitudinal phonons in the c direction in p-H_2. The instrumental widths are shown by the full curve.

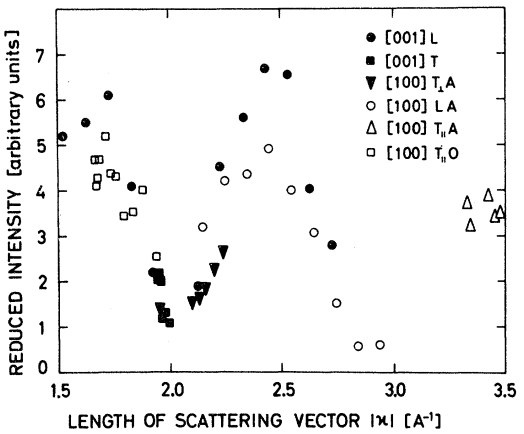

FIG. 11. Reduced intensities of the measured neutron groups in p-H_2, shown for the dispersion curves for which the inelastic structure factor varies slowly with $\vec{\kappa}$. The open and the full signatures correspond to data measured on two different crystals, and the intensities differ by an unknown factor. If the harmonic approximation is applied the reduced intensities would be independent of $\vec{\kappa}$.

proximated to Gaussians, and we have subtracted an extrapolated smooth background. Figure 9 shows the estimated width of the neutron groups. Figure 10 shows some neutron groups measured along a boundary of the Brillouin zone. These were measured with a fixed monochromator energy of 14.6 meV.

The integrated intensities of the measured neutron groups vary rather dramatically. By approximating the groups to Gaussians we have estimated the integrated intensities. These are then corrected for the variation in the instrumental sensitivity and for the factor

$$f = j_0^2(\kappa d/2)\,(k/k_0)\,e^{-2W} g_j^2(\vec{q}, \vec{\tau}) \quad ,$$

where g_j^2 is the inelastic structure factor[10] given as

$$g_j^2(\vec{q}, \vec{\tau}) = \frac{1}{M\omega_j(\vec{q})} \left| \sum_s \vec{\xi}_{sj} \cdot \vec{\kappa}\, e^{(\vec{\tau}\cdot\vec{r}_s)} \right|^2 \quad ,$$

and e^{-2W} is the Debye–Waller factor. $\vec{\tau}$ is a reciprocal lattice vector, $\vec{\xi}_{sj}$ is the normalized eigenvector of the sth molecule in the unit cell in the jth mode of vibration, $\vec{r}_s$ is the position vector of the sth molecule within the unit cell, $\vec{q}$ is the wave vector, and $\omega_j(\vec{q})$ is the energy of the phonon. The Debye–Waller factor is obtained from the incoherent scattering experiment described below, and the inelastic structure factor is calculated using the polarization vectors determined by the Born–von Karman calculation. The reduced intensities so obtained would be constant if the harmonic approximation applied, and Fig. 11 shows the result observed for those scans, where the inelastic structure factor varies slowly. The open and the full signatures correspond to results obtained with two different crystals and the two sets of data differ by an unknown scaling factor. The observed strong variation in the reduced intensities is ascribed to quantum and anharmonic effects. However, the results must be considered as preliminary on account of the uncertain background extrapolation and because the line shape is assumed Gaussian. The natural scattering profile for the high-energy phonons may have long wings of low

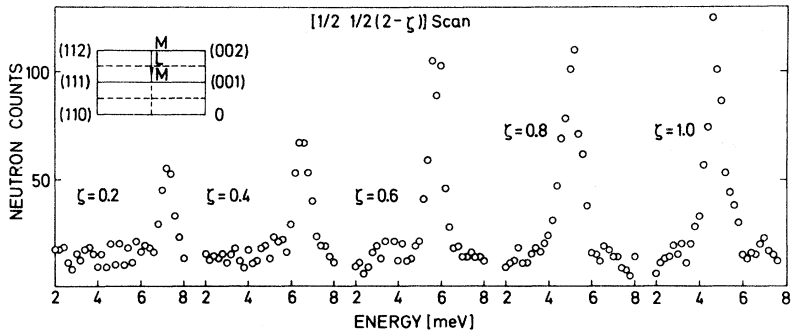

FIG. 10. Typical neutron groups measured in p-H_2 in Brillouin-zone boundary scans.

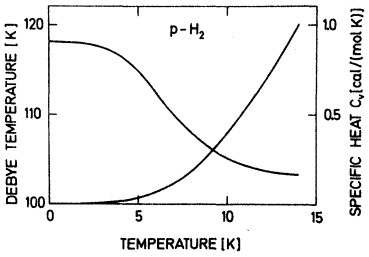

FIG. 12. Specific heat and Debye temperature for p-H_2 calculated by using the effective force constants.

intensity[12] but a very substantial reduction in the neutron scattering background is needed before such line shapes can be measured.

The effective force constants determined in the Born–von Karman fit are shown in Table III. These constants have been used to calculate a density-of-states function, the elastic constants, the sound velocities, the compressibility, the specific heat, and the Debye temperature, which are shown in Fig. 12. Specific-heat measurements on very pure p-H_2 in the temperature range 0.5–5 K have been made by Robert and Daunt,[13] and they find the Debye temperature $\Theta_D(0) = 122$ K. Wanner and Meyer[14] have measured the sound velocities in single crystals of normal hydrogen, and he finds $\Theta_D(0) = 111$ K.

The transverse-optic phonon mode in p-H_2 has been studied with Raman scattering by Silvera, Hardy, and McTague.[6] They find the energy of the phonons with zero wave vector to be $\epsilon_{TO}(0) = 4.685$ meV, in agreement within our experimental accuracy with our value $\epsilon_{TO}(0) = 4.62 \pm 0.10$ meV.

The measured phonon energies in p-H_2 can be compared with the theoretical calculations of Klein and Koehler[4] and of Biem and Mertens.[5] Klein and Koehler perform a self-consistent phonon calculation using a Lennard-Jones potential and a short-range correlation function as given by (1). As for o-D_2 the measured[8] phonon energies are in better agreement with the self-consistent frequencies $\omega_{\vec{q}}$ than with the inverse eigenvalues $\Omega_{\vec{q}}$ of the displacement-correlation function (Ref. 4). For phonons with wave vectors in the c direction there is complete agreement between the longitudinal phonon energies and $\omega_{\vec{q}}$, whereas the theoretical value of $\Omega_{\vec{q}}$ are 35% too high. For the transverse phonons in the same direction, $\omega_{\vec{q}}$ are 5% below, and $\Omega_{\vec{q}}$ 5% above the measured dispersion curve. Biem and Mertens[5] apply a random-phase approximation using a Lennard-Jones potential, but introduce two parameters in the short-range correlation function. Good agreement is obtained with our measured values, if all the calculated energies are multiplied by 1.3.

C. Debye-Waller Factor in Solid p-H_2

The differential neutron scattering cross sections are proportional to the Debye–Waller factor $e^{-2W} = \langle e^{i\vec{\kappa}\cdot\vec{u}} \rangle^2$, where $\vec{\kappa}$ is the scattering vector and $\vec{u}$ is the displacement of a molecule from its lattice point. In the harmonic approximation we have $e^{-2W} = e^{-\langle(\vec{\kappa}\cdot\vec{u})^2\rangle} = e^{-\kappa^2\langle u^2\rangle/3}$ if we assume the anisotropy to be small. At temperatures small compared to the Debye temperature we have

$$\langle u^2 \rangle = \frac{\hbar}{2NM} \sum_{\vec{q}} \frac{1}{\omega_{\vec{q}}} \ .$$

$\langle u^2 \rangle$ may be calculated using the density-of-states function determined by the effective force constants, and we find $\langle u^2 \rangle = 0.46$ Å^2. However, a convenient method of determining the Debye–Waller factor in p-H_2 is to measure the incoherent $J=0$ to $J=1$ neutron scattering intensity. Equation (3) shows that when $\omega = E_{J'} - E_J$, we observe for p-H_2 an incoherent scattering peak, which corresponds to the quasielastic incoherent scattering in a monoatomic solid. When $J' = 1$ and $J = 0$ the intensity of this scattering varies with κ as $j_1^2(\frac{1}{2}\kappa d)e^{-2W}$ and the natural width of the scattering peak, which is determined by the rotational anisotropy of a $J=1$ molecule in a pure $J=0$ crystal, is extremely small.

We have used this incoherent scattering to determine the dependence of the Debye–Waller factor on $\vec{\kappa}$ by measuring the integrated intensity in constant $\vec{\kappa}$ scans on a triple-axis spectrometer. This method has the following advantages: The scattering intensity is high, there is no multiple scattering,

TABLE III. Third-nearest-neighbor force model for p-H_2 at 5.4 K and zero pressure. The corresponding o-D_2 data are shown in parenthesis.

Force constants (dyn/cm)		Elastic constants (10^8 dyn/cm^2)		Sound velocities (10^3 m/sec)	
α_1	36 (63)	C_{11}	42 (82)	v_L^z	2.40 (2.25)
β_1	−6 (−9)	C_{12}	18 (29)	v_T^z	1.11 (1.07)
γ_1	66 (127)	C_{33}	51 (102)	v_L^{xy}	2.17 (2.02)
δ_1	35	C_{44}	11 (23)	v_T^{xy}	1.17 (1.14)
α_2	4 (6)	C_{13}	5 (9)		
β_2	93 (174)	B	21 (40)		
γ_2	−4 (−9)				
ϵ_2	20 (11)				
α_3	1 (−2)				
β_3	−2 (4)				
γ_3	0 (1)				
δ_3	2				

and no correction is needed for extinction or for variation in instrumental sensitivity provided that the incoming neutron energy is below twice the rotational energy $E_1 - E_0$. The corrections due to incoherent phonon scattering can be kept small when a high instrumental energy resolution is used.

The results are shown in Fig. 13. The sample was a single crystal of p-H_2 at $T = 5.4$ K, and we have measured the Debye–Waller factor $e^{-\langle(\vec{\kappa}\cdot\vec{u})^2\rangle}$ for $\vec{\kappa}$ in the [001] and in the [100] directions. The lower points in Fig. 13 show the measured intensities. A scaling factor is applied to each set of data so that, when corrected for the Bessel function, the data extrapolates to unity as κ^2 goes to zero. Within the experimental accuracy $2W$ is a linear function of κ^2, as expected, if the self-correlation function $G_s(\vec{r}, \infty)$ for the molecules is described by a Gaussian probability function, as in the harmonic approximation. Further there is no significant difference between the Debye–Waller factor in the two crystallographic directions. For both directions we find $\langle u^2\rangle = 0.48 \pm 0.03$ Å^2. This means that the thermal amplitudes of the zero-point motion of the molecules are equal in the two directions within our experimental accuracy, and they agree with the value calculated by means of the effective force constants, which are determined by the coherent phonon measurements.

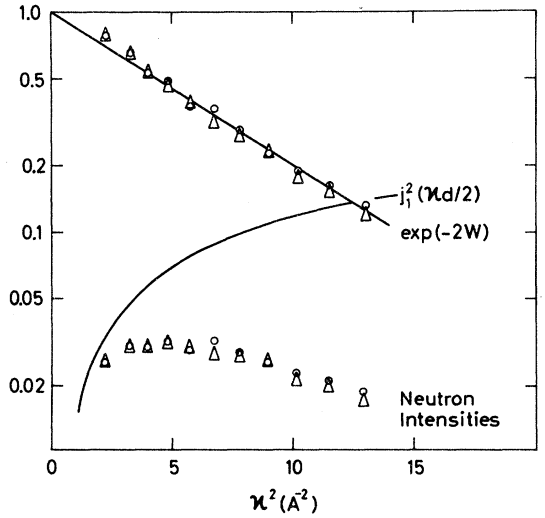

FIG. 13. Debye–Waller factor for p-H_2 at 5.4 K determined by incoherent neutron scattering. The lower points in the figure show the intensity of the $J = 0$ to $J = 1$ scattering with no energy exchange with the lattice. This intensity is proportional to the Bessel function squared $j_1^2(\frac{1}{2}\kappa d)$ and to the Debye–Waller factor e^{-2W}. The sample is a single crystal and the measurements are performed with the wave vector $\vec{\kappa}$ in the [001] direction (circles) and in the [100] direction (triangles). The intensities are multiplied with a scaling factor so that, when divided by $j_1^2(\frac{1}{2}\kappa d)$, the data extrapolates to unity as κ^2 goes to zero in the logarithmic plot. From the slope of the line e^{-2W} vs κ^2 the mean-square displacement of the molecules is found and for κ in both directions we find $\langle u^2\rangle = 0.48 \pm 0.03$ Å^2.

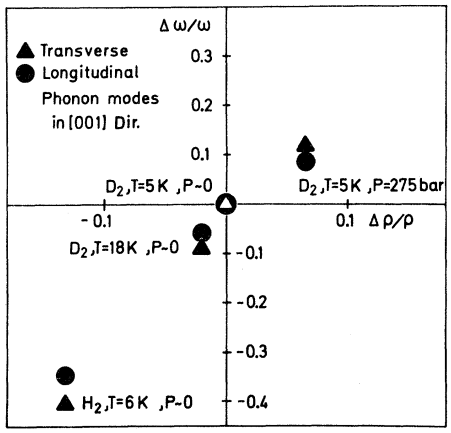

FIG. 14. Variation of the phonon energies with density. The energies are averaged over the transverse and longitudinal branches in the c direction. The figure shows how these phonon energies vary when the density is changed either by applying pressure or by raising the temperature. Results for hydrogen are also included in the figure. To account for the mass difference the phonon energies of hydrogen are divided by $\sqrt{2}$.

IV. CONCLUSIONS

Our measurements of the phonon dispersion relations in solid o-D_2 and p-H_2 are generally in good agreement with theory, provided that the quantum effects are explicitly taken into account. The measured energies are somewhat lower than those calculated from the displacement correlation function by Klein and Koehler[4] and those calculated by Biem and Mertens.[5] The discrepancy is as large as 30–40% at the highest energies. On the other hand, the experimental dispersion relations for both o-D_2 and p-H_2 are in rather close agreement with the self-consistent phonon frequencies $\omega_{\vec{q}}$ in the calculation of Klein and Koehler.[4]

The Born–von Karman analysis of the experimental results reveals that the phonon energies are essentially entirely determined by the effective nearest-neighbor bond-stretching forces. The sound velocities and the heat capacity have been deduced from the analysis for both isotopes. Incoherent neutron scattering has allowed an accurate determination of the Debye–Waller factor in p-H_2 and this also agrees well with the value calculated from the phonon energies, although the justification for the use of such an analysis for quantum crystals is not immediately clear.

Although the isotopic mass of hydrogen is only one-half that of deuterium and the intermolecular potentials are almost identical, the phonon energies in the solids are very similar, as is apparent from

the Debye temperatures of 114 and 118 K for o-D_2 and p-H_2, respectively. The increased zero-point vibrations in H_2 expand the crystal so that the effective-force constants are substantially softened, and this almost cancels the effect of the mass difference.

The average shift in the transverse and longitudinal phonon energies in the c direction is shown as a function of the change in density in Fig. 14. For a given density change, temperature causes about twice as great a change in the phonon energies as does pressure. The transverse phonon energies are more sensitive to density changes than are the longitudinal phonons. Results for solid hydrogen have also been included in Fig. 14. The phonon energies of hydrogen have been divided by $\sqrt{2}$ to account for the mass difference.

All our experimental results can be accounted for in a satisfactory way by the conventional harmonic phonon theory and the associated force constants determined by the Born–von Karman calculations, except for the phonon scattering intensities for hydrogen shown in Fig. 11. These are in strong disagreement with the one-phonon scattering cross section in the harmonic approximation, including the Debye–Waller factor determined by incoherent scattering. Similar but less pronounced effects were observed in deuterium. An oscillatory variation of the intensity has also been observed[15] in neutron scattering experiments on solid helium. The scattering function $S(\kappa, \omega)$ for quantum solids has recently been considered by Horner,[16] who finds that the interference between one- and two-phonon processes can give rise to an oscillatory intensity variation similar to that shown in Fig. 11. It seems, therefore, that the only pronounced qualitative manifestation of quantum effects in neutron scattering from quantum crystals is the anomalous variation of the scattered intensity.

ACKNOWLEDGMENTS

We are grateful to H. Bjerrum Møller, A. R. Mackintosh, K. Carneiro, and B. Powell for stimulating discussions. Further, we acknowledge the very competent technical assistance of J. Z. Jensen.

[1]See the review by N. R. Werthamer, Am. J. Phys. **37**, 763 (1969), and references therein.

[2]V. J. Minkiewicz, T. A. Kitchens, F. P. Lipschultz, R. Nathans, and G. Shirane, Phys. Rev. **174**, 267 (1968); R. A. Reese, S. K. Sinha, T. O. Brun, and C. R. Tilford, Phys. Rev. A **3**, 1688 (1971).

[3]L. H. Nosanow, Phys. Rev. **146**, 126 (1966).

[4]M. L. Klein and R. Koehler, J. Phys. C **3**, L102 (1970); Phys. Lett. A **33**, 253 (1970).

[5]W. Biem and F. G. Mertens (private communication); F. G. Mertens, Institute für Festkörperforschung Report No. Jül-734-FF, 1971 (unpublished).

[6]J. F. Silvera, W. N. Hardy, and J. P. McTague, Discuss. Faraday Soc. **48**, 54 (1969); Phys. Rev. B **5**, 1578 (1972).

[7]W. Schott, Z. Phys. **231**, 243 (1970); H. Stein, R. Stockmeyer, and H. Stiller, in *Proceedings of the International Conference on Phonons, Rennes, France, 1971*, edited by M. A. Nusimovici (Flammarion, Paris, 1971), p. 223.

[8]M. Nielsen and H. Bjerrum Møller, Phys. Rev. B **3**, 4383 (1971).

[9]G. Sarma, in *Inelastic Scattering of Neutrons in Solids and Liquids* (IAEA, Vienna, 1961), p. 397.

[10]J. C. Gylden Houmann and R. M. Nicklow, Phys. Rev. B **1**, 3943 (1970).

[11]J. P. Franck and R. Wanner, Phys. Rev. Lett. **25**, 345 (1970).

[12]H. R. Glyde and F. C. Khanna, Can. J. Phys. **49**, 23 (1971).

[13]R. J. Robert and J. G. Daunt, J. Low Temp. Phys. **6**, 97 (1972).

[14]R. Wanner and H. Meyer, Phys. Lett. A **41**, 189 (1972).

[15]T. A. Kitchens, G. Shirane, V. J. Minkiewicz, and E. B. Osgood, Phys. Rev. Lett. **29**, 552 (1972).

[16]H. Horner, Phys. Rev. Lett. **29**, 556 (1972).